Contribution from UA CNRS 322, Laboratoire de Chimie, Photochimie et Electrochimie Moléculaires, Equipe de Chimie Inorganique Moléculaire, Université de Bretagne Occidentale, 29287 Brest Cédex, France, and URA CNRS 804, Laboratoire de Physique Cristalline, Université de Rennes I, 35042 Rennes Cédex, France

Interconversion of Mononuclear and Quadruply Bonded Dinuclear Dibenzotetraaza[14]annulene Complexes of Molybdenum

Jean Marc Giraudon,[1a] Jean Sala-Pala,*[,1a] Jacques E. Guerchais,*[,1a] and Loïc Toupet[1b]

Received May 22, 1990

Several aspects of the chemistry of the previously reported dinuclear molybdenum(II) complexes **1** ($[\{Mo(R_2C_{22}H_{20}N_4)\}_2]$), in which the substituted dibenzotetraaza[14]annulene ligand adopts its usual tetradentate coordination mode, have been developed. Under a dinitrogen atmosphere, complexes **1** react with TCNE (TCNE:**1** = 1) in acetonitrile at room temperature to afford the corresponding diradical complexes **2** ($[\{Mo(R_2C_{22}H_{20}N_4)\}_2]^{\bullet+}TCNE^{\bullet-}$). Under different conditions (TCNE:**1** = 4, presence of air) the same reactants give the mononuclear oxomolybdenum(V) complexes **3**, $[MoO(R_2C_{22}H_{20}N_4)][C_3(CN)_5]$. The oxocation and the 1,1,2,3,3-pentacyanopropenide anion of **3** clearly arise from reaction of **2** with dioxygen or water. The redox properties of **3** have been examined electrochemically and chemically. While chemical reduction of **3a** (R = H) with cobaltocene affords the corresponding oxomolybdenum(IV) complex **4a** ($[MoO(R_2C_{22}H_{20}N_4)]$), reduction with Na-Hg gives the multiply bonded dimolybdenum radical anion **1a**$^{\bullet-}$ ($[\{Mo(R_2C_{22}H_{20}N_4)\}_2]^{\bullet-}$) (R = H). X-Band ESR spectra of complexes **3** have been recorded at room temperature and 140 K, showing interaction of the unpaired electron with the Mo nucleus. A detailed analysis of spin-Hamiltonian parameters is given, and the bonding is discussed, assuming that the ligand field around molybdenum has C_{2v} symmetry. The structure of **3a** (R = H) has been determined by single-crystal X-ray diffraction analysis. The black-green crystals are triclinic, space group $P\bar{1}$ with a = 9.057 (5) Å, b = 12.327 (4) Å, c = 14.939 (5) Å, α = 103.69 (7)°, β = 102.54 (9)°, γ = 96.31 (8)°, V = 1558 (2) Å^3, and Z = 2. The structure was solved by using 3168 independent reflections. Refinement, carried out with anisotropic thermal parameters for all non-H atoms, converged to an unweighted R value of 4.8% and a weighted R value of 4.3%. The molybdenum atom has a square-pyramidal coordination with the oxygen atom in an apical position [MoO = 1.670 (3) Å; MoN = 2.034 (4)-2.041 (4) Å]. The geometry of the $[C_3(CN)_5]$ anion is approximately C_{2v}.

Introduction

Unbridged dimers in which two metal centers are associated with two tetradentate ligands to give the $[ML_4]_2$ stoichiometry represent a special class of metal-metal-bonded complex. One of the striking features of this class, which has been developed mainly with porphyrin ligands, is the ability to accommodate different formal bond multiplicities to give compounds that are virtually isostructural.

In the case of the neutral metalloporphyrin complexes $[M(porph)]_2$, the formal metal-metal bond order clearly depends on the electronic configuration of the metal; it varies from 1 for group 9 metals (Rh, Ir)[2,3] to 2 for group 8 metals (Ru, Os),[4,5] 3 for rhenium, and 4 for group 6 metals (Mo, W).[5,6] Modification of the bond order may be obtained by oxidation. Thus, controlled chemical oxidation of the doubly bonded dimers $[M(porph)]_2$ (M = Ru, Os) clearly generated the $M^{II}M^{III}$ mixed-valence cationic complexes and the $M^{III}M^{III}$ dicationic complexes.[7] The reactivities of these metalloporphyrin dimers reflect, as expected, the differences in the metal-metal bond order. While cleavage of the metal-metal bond is quite common with metals belonging to groups 8 and 9,[2,8] access to a mononuclear complex has never been reported for molybdenum and tungsten. With molybdenum, a few examples of $[ML_4]_2$ complexes have been described recently. The first was reported by Collman et al., who obtained the porphyrin complex $[\{Mo(porph)\}_2]$ by heating in vacuo the mononuclear species $[Mo(porph)(C_6H_5C{\equiv}CC_6H_5)]$.[5] Binuclearity was established by mass spectroscopy while variable-temperature ^1H NMR studies provided evidence for both the existence of a quadruple bond and for a barrier to rotation about the metal-metal bond.[5] Subsequently, confirmation of this structure [Mo$\overset{4}{-}$Mo = 2.239 (1) Å] was obtained by an X-ray study.[9] It is noteworthy that this compound, and not [MoO(OH)(porph)] as thought for 15 years,[10] is actually the first product obtained from the reaction of $[Mo(CO)_6]$ with H_2porph, formation of the oxomolybdenum (V) complex occurring only during the chromatographic purification stage.[9] Using a dibenzotetraaza[14]annulene ligand,[11] we recently showed that reaction of $[Mo_2(acet)_4]$ with Li_2L_4 (L_4^{2-} = $C_{22}H_{22}N_4^{2-}$, Figure 1 afforded the quadruply metal-metal-bonded complex $[ML_4]_2$. Access to mixed-valence $Mo^{II}Mo^{III}$ and $Mo^{I}Mo^{II}$ species was achieved chemically and electrochemically and the $Mo^{II}Mo^{III}$ dimer fully characterized by ESR and X-ray diffraction [Mo$\overset{3.5}{-}$Mo = 2.221 (1) Å].[12] Finally, Floriani et al.[13] reported that the dichloromolybdenum(IV) complex $[MoCl_2L_4]$ (L_4^{2-} = $C_{12}H_{18}N_2O_2^{2-}$), when treated with sodium in presence of diphenylacetylene, yielded the diamagnetic dimer $[ML_4]_2$ [Mo$\overset{4}{-}$Mo = 2.1678 (4) Å]. In contrast with the reactivities of the group 8 and 9 metal dimers $[ML_4]_2$, those of the above mentioned molybdenum complexes have been very little investigated. We now report the results of a study of the reactions between the $[\{Mo(R_2C_{22}H_{20}N_4)\}_2]$ (Mo$\overset{4}{-}$Mo) complexes and tetracyanoethene (TCNE) in which formation of mononuclear species occurs under certain conditions.

Experimental Section

All reactions were performed in Schlenk tubes in a dry oxygen-free nitrogen atmosphere. Solvents were distilled by standard techniques and thoroughly deoxygenated before use. Elemental analyses were performed

(1) (a) Université de Bretagne Occidentale. (b) Université de Rennes I.
(2) (a) Ogoshi, H.; Setsune, J.; Yoshida, Z. *J. Am. Chem. Soc.* **1977**, *99*, 3869. (b) Wayland, B. B.; Newman, A. R. *Inorg. Chem.* **1981**, *20*, 3093.
(3) Del Rossi, K. J.; Wayland, B. B. *J. Chem. Soc., Chem. Commun.* **1986**, 1653.
(4) (a) Collman, J. P.; Barnes, C. E.; Collins, T. J.; Brothers, P. J. *J. Am. Chem. Soc.* **1981**, *103*, 7030. (b) Collman, J. P.; Barnes, C. E.; Sweptson, P. N.; Ibers, J. A. *J. Am. Chem. Soc.* **1984**, *106*, 3500.
(5) (a) Collman, J. P.; Barnes, C. E.; Woo, L. K. *Proc. Natl. Acad. Sci. U.S.A.* **1983**, *80*, 7684. (b) Collman, J. P.; Woo, L. K. *Proc. Natl. Acad. Sci. U.S.A.* **1984**, *81*, 2592.
(6) Collman, J. P.; Garner, J. M.; Woo, L. K. *J. Am. Chem. Soc.* **1989**, *111*, 8141.
(7) Collman, J. P.; Prodoliet, J. W.; Leidner, C. R. *J. Am. Chem. Soc.* **1986**, *108*, 2916.
(8) (a) Setsune, J. I.; Yoshida, Z. I.; Ogoshi, H. *J. Chem. Soc., Perkin Trans. 1* **1982**, 983. (b) Collman, J. P.; Brothers, P. J.; McElwee-White, L.; Rose, E.; Wright, L. J. *J. Am. Chem. Soc.* **1985**, *107*, 4570. (c) Sishta, C.; Ke, M.; James, B. R.; Dolphin, D. *J. Chem. Soc., Chem. Commun.* **1986**, 787. (d) Paonessa, R. S.; Thomas, N. C.; Halpern, J. *J. Am. Chem. Soc.* **1985**, *107*, 4333. (e) Wayland, B. B.; Coffin, V. L.; Farnos, M. D. *Inorg. Chem.* **1988**, *27*, 2745. (f) James, B. R.; Pacheco, A.; Rettig, S. J.; Ibers, J. A. *Inorg. Chem.* **1988**, *27*, 2414.
(9) Yang, C. H.; Dzugan, S. J.; Goedken, V. L. *J. Chem. Soc., Chem. Commun.* **1986**, 1313.
(10) Fleischer, E. B.; Srivastava, T. S. *Inorg. Chim. Acta* **1971**, *5*, 151.
(11) (a) Jäger, E. G. *Z. Anorg. Allg. Chem.* **1969**, *364*, 177. (b) L'Eplattenier, F. A.; Pugin, A. *Helv. Chim. Acta* **1975**, *58*, 917. (c) Goedken, V. L.; Weiss, M. C. *Inorg. Synth.* **1980**, *20*, 115.
(12) Mandon, D.; Giraudon, J. M.; Toupet, L.; Sala-Pala, J.; Guerchais, J. E. *J. Am. Chem. Soc.* **1987**, *109*, 3490.
(13) Pennesi, G.; Floriani, C.; Chiesi-Villa, A.; Guastini, C. *J. Chem. Soc., Chem. Commun.* **1988**, 350.

0020-1669/91/1330-0891$02.50/0

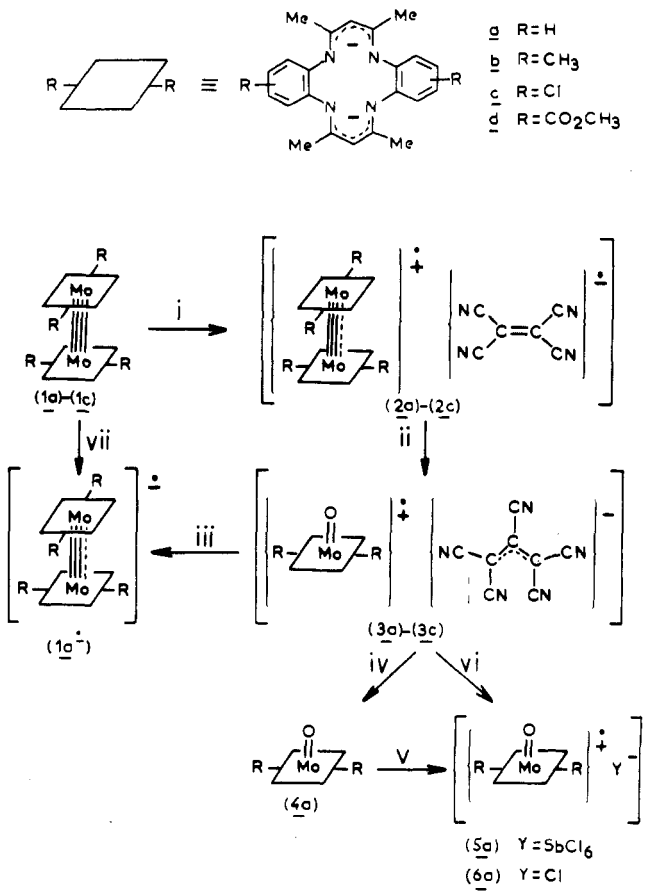

Figure 1. Top: Dibenzotetraaza[14]annulene ligands $(R_2C_{22}H_{20}N_4)^{2-}$. Key (throughout the work): a, R = H; b, R = CH_3; c, R = Cl; d, R = CO_2CH_3. Bottom: Synthesis of the molybdenum complexes. Key: (i) TCNE [TCNE:**1** = 1], CH_3CN, room temperature (90%); (ii) excess TCNE and water or dioxygen, CH_3CN, room temperature (70%); (iii) Na–Hg, THF, room temperature; (iv) $[Co(C_5H_5)_2]$, THF, room temperature (ca. quantitative); (v) $[(BrC_6H_4)_3N]Y$ (**5a**, Y = $SbCl_6$), THF, room temperature (80%); (vi) HY gas (**6a**, Y = Cl), THF, −20 °C (88%); (vii) Na–Hg, toluene, −10 °C (see ref 12).

by Service Central d'Analyse du CNRS, Vernaison, France.

^1H NMR spectra were obtained with a Brucker AM 300 spectrometer (330.13 MHz, FT). Chemical shifts were measured by using TMS as internal reference.

ESR spectra were obtained by using a Jeol FE 3X spectrometer (X-band); the computer program used for the simulation of the frozen-solution spectra has been previously described.[14]

The apparatus, the three-compartment microelectrochemical cell, the treatment of the solvent, and the supporting electrolyte for the electrochemical studies have all been previously described.[15,16] The reference electrode used is the half-cell = Pt/ferrocenium picrate (10^{-2} M), ferrocene (10^{-2} M), Bu_4NPF_6 (0.2 M), and benzonitrile. For comparison of the present results with other work, the Fc^+/Fc formal potential has been measured versus SCE in benzonitrile (0.2 M Bu_4NPF_6) $E'_0(Fc^+/Fc)$ = +0.43 V vs SCE.

UV–visible spectra were obtained on a Cary 219 (Varian) spectrometer. IR spectra were run by using a Perkin-Elmer 1430 spectrophotometer and KBr pellets.

TCNE was purified prior to use by vacuum sublimation (10^{-1} mmHg; 70 °C). Tris(4-bromophenyl)ammonium hexachloroantimonate was purchased from Aldrich and used without further purification. The $C_{22}H_{24}N_4$ ligand was prepared as previously described by Jäger and Goedken.[11] The substituted $R_2C_{22}H_{22}N_4$ ligands (R = Cl, CH_3, CO_2Me) were prepared by a similar method starting from 2,4-pentanedione and the corresponding 4-R-*o*-phenylenediamine. In the cases where R does not equal H, the ligand may exist as two isomeric forms according to the relative positions of the R groups[11b] but we were unable to obtain information on this point from ^1H NMR data. The starting dinuclear complexes **1** ($[\{Mo(R_2C_{22}H_{20}N_4)\}_2]$) (**1a**, R = H; **1b**, R = CH_3; **1c**, R = Cl) were synthesized as previously described[12] but access to the R = CO_2Me analogue **1d** was not possible. The tetracarbonyl complexes $[M(CO)_4(R_2C_{22}H_{22}N_4)]$ (M = Mo, R = CO_2Me; M = W, R = H) were prepared by the literature methods.[17] Data for the molybdenum complex are as follows. Anal. Calcd for $MoC_{30}H_{28}N_4O_4$: C, 53.9; H, 4.2; N, 8.4. Found: C, 53.9; H, 4.4; N, 8.2. IR (KBr, cm^{-1}): 2000 m, 1890 sh, 1875 s, 1840 s [ν(CO)]. ^1H NMR ($CDCl_3$): δ 2.20 (6 H, s, CH_3), 3.40 (2 H, s, CH_2), 3.92 (6 H, s, CO_2CH_3), 4.90 (1 H, s, CH), 7.90 (8 H, m, ArH), 12.75 (1 H, s, NH).

Complexes 2 ($[\{Mo(R_2C_{22}H_{20}N_4)\}_2]^{+\bullet}TCNE^{-\bullet}$) (2a, R = H; 2b, R = CH_3; 2c, R = Cl). 2a. A suspension of **1a** ($[\{Mo(C_{22}H_{22}N_4)\}_2]$) (1.00 g, 1.14 mmol) in acetonitrile (50 mL) was stirred with TCNE (0.146 g, 1.14 mmol) at room temperature, the color changing immediately from dark brown to brown. After 3 h, the solvent was removed under reduced pressure, and then the residue was extracted with dichloromethane and filtered twice on Celite. The resulting solution was concentrated, and addition of pentane gave **2a** as a brown-red powder (ca. 90%). Anal. Calcd for $Mo_2C_{50}H_{44}N_{12}\cdot 0.5CH_2Cl_2$: C, 57.9; H, 4.3; N, 16.0; Mo, 18.3. Found: C, 57.6; H, 4.6; N, 15.1; Mo, 17.4. IR (KBr, cm^{-1}): 2183 s, 2144 m [ν(CN)]. ESR (CH_3CN, room temperature): cation, central signal (I_{Mo} = 0), g = 1.958 with a six-line spectrum (I_{Mo} = $^5/_2$), A_{Mo} = 35.2 G; anion, nine-line spectrum, g = 2.003, A_N = 1.56 G.

Complexes **2b** and **2c** were prepared analogously to **2a** from the corresponding dinuclear complexes **1**.

Complexes 3 ($[MoO(R_2C_{22}H_{20}N_4)][C_3(CN)_5]$) (3a, R = H; 3b, R = CH_3; 3c, R = Cl). 3a. A suspension of **1a** ($[\{Mo(C_{22}H_{22}N_4)\}_2]$) (0.30 g, 0.34 mmol) in acetonitrile (20 mL) was stirred (5 h, room temperature) with an excess of TCNE (0.180 g, 1.37 mmol) in the presence of air; the color changed from dark brown to green. The solvent was evaporated and the residue extracted with dichloromethane. After two filtrations on Celite, the solvent was removed under reduced pressure, and the resulting green powder was washed with pentane and dried under vacuum (ca. 70%). Similar experiments under a dinitrogen atmosphere affords impure samples of this complex. Anal. Calcd for $MoOC_{30}H_{22}N_9\cdot 0.5CH_2Cl_2$: C, 55.2; H, 3.5; N, 19.0. Found: C, 54.8; H, 3.4; N, 19.9. IR (KBr, cm^{-1}): 2195 s [ν(CN)], 950 s [ν(MoO)]. ESR (CH_3CN, room temperature): central signal (I_{Mo} = 0), g = 1.958 with a six-line spectrum (I_{Mo} = $^5/_2$), A_{Mo} = 34.9 G.

Complexes **3b** and **3c** were prepared in a similar manner from the corresponding $[\{Mo(R_2C_{22}H_{20}N_4)\}_2]$ (**1**) complexes. Data for **3b** are as follows. Anal. Calcd for $MoOC_{32}H_{26}N_9$: C, 59.2; H, 4.1; N, 19.4. Found: C, 58.7; H, 4.3; N, 18.7. IR (KBr, cm^{-1}): 2200 s [ν(CN)]; 950 [ν(MoO)]. Data for **3c** are as follows. Anal. Calcd for $MoOC_{30}H_{20}N_9Cl_2$: C, 52.2; H, 3.0; N, 18.3. Found: C, 52.2; H, 3.1; N, 17.3. IR (KBr, cm^{-1}): 960 m [ν(MoO)].

Complex 4a ($[MoO(R_2C_{22}H_{20}N_4)]$) (R = H). To a solution of cobaltocene $[Co(\eta\text{-}C_5H_5)_2]$ (0.18 g, 0.95 mmol) in THF (20 mL) was added a solution of $[MoO(C_{22}H_{22}N_4)][C_3(CN)_5]$ (**3a**) (0.59 g, 0.95 mmol) in THF (50 mL). The solution was stirred in the dark (6 h, room temperature) and then evaporated to dryness. After the residue was washed with pentane, extraction with a toluene–dichloromethane (1:1) mixture gave a red solution. Concentration gave yellow microcrystals in an almost quantitative yield. Complex **4a** is very air-sensitive, especially in solution. ^1H NMR (CD_2Cl_2): δ 2.11 (12 H, s, CH_3), 4.90 (2 H, s, CH), 6.98 (8 H, s, C_6H_4). IR (KBr, cm^{-1}): 940 s [ν(MoO)].

Complex 5a ($[MoO(R_2C_{22}H_{20}N_4)][SbCl_6]$) (R = H). To a Schlenk tube containing $[(BrC_6H_4)_3N][SbCl_6]$ (0.35 g, 0.41 mmol) was transferred, in the dark, a THF (20 mL) solution of $[MoO(C_{22}H_{22}N_4)]$ (**4a**) (0.19 g, 0.41 mmol). After the mixture was stirred (3 h, room temperature), the green precipitate was filtered and washed with pentane and then toluene. Extraction with dichloromethane gave a green solution that was filtered twice on Celite. Evaporation to dryness gave a green powder (ca. 80%). ESR (CH_3CN, room temperature): central signal (I_{Mo} = 0), g = 1.957 with a six-line spectrum (I_{Mo} = $^5/_2$), A_{Mo} = 35.2 G. IR (KBr, cm^{-1}): 955 s [ν(MoO)].

Complex 6a ($[MoO(R_2C_{22}H_{20}N_4)]Cl$) (R = H). Dry HCl gas was bubbled through a THF solution (150 mL) of $[MoO(C_{22}H_{22}N_4)][C_3(CN)_5]$ (**3a**) (0.50 g, 0.08 mmol) for 1 h at −20 °C. The solvent was evaporated and the residue washed with hexane and then extracted with dichloromethane. The resulting solution was filtered twice on Celite. Concentration gave a green powder, which was washed with hexane and then dried (88%). ESR (1:1 toluene–acetone mixture, room temperature): g = 1.958, A_{Mo} = 38.0 G. IR (KBr, cm^{-1}): 960, m [ν(MoO)]. CV (C_6H_5CN, 0.1 M Bu_4NPF_6, 200 mV·s^{-1}): $E_{1/2}$ = −0.73 and 0.44 V vs Fc^+/Fc.

(14) (a) Vivien, D.; Gibson, J. F. *J. Chem. Soc., Faraday 2* **1975**, 1640. (b) Sanchez, C.; Vivien, D.; Livage, J.; Sala-Pala, J.; Viard, B.; Guerchais, J. E. *J. Chem. Soc., Dalton Trans.* **1981**, 64.
(15) Le Mest, Y.; L'Her, M.; Courtot-Coupez, J.; Collman, J. P.; Evitt, E. R.; Bencosme, C. S. *J. Electroanal. Chem. Interfacial Electrochem.* **1985**, *184*, 331.
(16) Giraudon, J. M.; Mandon, D.; Sala-Pala, J.; Guerchais, J. E.; Kerbaol, J. M.; Le Mest, Y.; L'Haridon, P. *Inorg. Chem.* **1990**, *29*, 707.

Table I. Crystal and Refinement Data for $[MoO(C_{22}H_{22}N_4)][C_3(CN)_5]\cdot CH_2Cl_2$ (**3a**)

A. Crystal Data

formula	$[C_{22}H_{22}MoN_4O]$-$[C_8N_5]\cdot CH_2Cl_2$	V, Å^3	1558 (2)
		Z	2
fw	703.4	d_{calcd}, g·cm^{-3}	1.50
cryst syst	triclinic	cryst size, mm	0.18 × 0.20 × 0.25
space group	$P\bar{1}$		
a, Å	9.057 (5)	radiation	Mo$K\alpha$(λ = 0.71069 Å)
b, Å	12.327 (4)		
c, Å	14.939 (5)	monochromator	graphite cryst
α, deg	103.69 (7)	abs coeff, cm^{-1}	6.2
β, deg	102.54 (9)	T, K	296
γ, deg	96.31 (8)	F(000)	714

B. Data Collection and Processing

scan method	ω–2θ	total no. of reflcn data	4213
$2\Theta_{max}$, deg	55		
t_{max} (for one measurement), s	60	no. of reflcns used	3168 [$I > 3\sigma(I)$]
octants collcd	$h,\pm k,\pm l$ ($h \le 13$, $k \le 14$, $l \le 15$)	R_{int}	0.009
		intens var, %	0.4

C. Treatment of Data

no. of params refined	468	final R^a with H	0.048
R(isotropic)	0.094	final R^b with H	0.043
R(anisotropic)	0.057	$S_w{}^c$	1.5

$^a R = \sum||\Delta F|/\sum F_o$. $^b R_w = [\sum w(\Delta F)^2/\sum F_o^2]^{1/2}$; weighting scheme $w = 1/\sigma(F_o^2) = [\sigma^2(I) + (0.04F_o^2)^2]^{-1/2}$. $^c S_w = [\sum w(\Delta F)^2/(N-P)^{1/2}$ with N = number of observations and P = number of parameters.

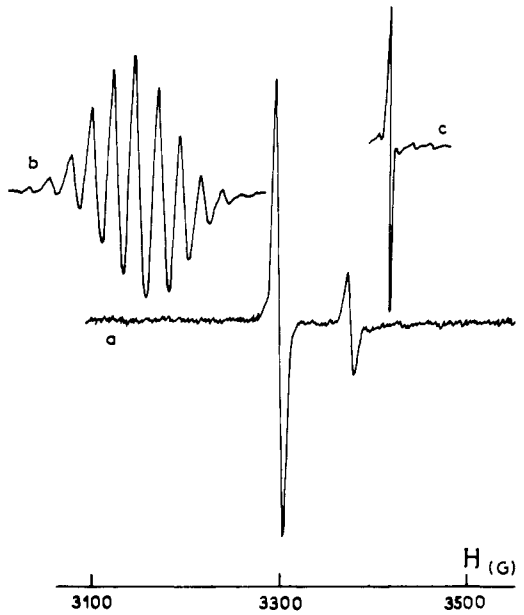

Figure 2. (a) ESR spectrum of the diradical complex **2a** ([[Mo($C_{22}H_{22}N_4$)]$_2$]$^{2+}$(TCNE)$^{\cdot-}$) (CH_3CN, room temperature). (b) Expansion of the signal assignable to the radical anion. (c) Expansion of the signal assignable to the radical cation.

Formation of the Oxocations $[MoO(R_2C_{22}H_{20}N_4)]^+$ (R = CO_2Me) and $[WO(R_2C_{22}H_{20}N_4)]^+$ (R = H). Both cations have been prepared by controlled-potential electrolyses (Mo, 0.40 V; W, 0.77 V vs. Fc^+/Fc) of benzonitrile solutions of the corresponding tetracarbonyl derivatives [M-$(CO)_4(R_2C_{22}H_{22}N_4)$],[17] as previously described for the R = H molybdenum analogue.[16] They have been fully characterized by CV and ESR studies (see Tables V and VI).

$[WO(C_{22}H_{22}N_4)]^+$: CV (C_6H_5CN, 0.1 M Bu_4NPF_6, 200 mV·s^{-1}): $E_{1/2}$ = −2.10, −0.75, and 0.25 V vs Fc^+/Fc; ESR (C_6H_5CN, 140 K): g_1 = 1.875, g_2 = 1.842, g_3 = 1.777 (see Figure 10).

Crystal Structure of 3a. X-ray Data Collection. A dark-green prismatic crystal obtained by recrystallization from dichloromethane–pentane was sealed in a glass capillary under dinitrogen and mounted on a Enraf Nonius CAD 4 diffractometer in a random orientation; the resulting crystal data and other structural details are quoted in Table I. The intensities of the half-reflection sphere were collected, measuring a reflection every hour as a check of the crystal and instrument stabilities.

(17) Dabrowiak, J. C.; Bell, L. G. *J. Chem. Soc., Chem. Commun.* **1975**, 512.

Table II. Final Positional Parameters and Equivalent Isotropic Displacement Parameters (Å^2) for $[MoO(C_{22}H_{22}N_4)][C_3(CN)_5]\cdot CH_2Cl_2$ (**3a**)^a

atom	x	y	z	B, Å^2
Mo(1)	0.19055 (6)	0.25915 (4)	−0.34501 (3)	2.603 (9)
Cl(1)	0.5079 (4)	0.1269 (2)	0.1735 (3)	11.5 (1)
Cl(2)	0.2220 (5)	−0.0014 (3)	0.0518 (2)	11.2 (1)
O	−0.0038 (4)	0.7348 (3)	0.3595 (3)	3.41 (9)
N(1)	0.2198 (5)	0.0982 (4)	−0.4037 (3)	2.9 (1)
N(2)	0.2811 (6)	0.2081 (4)	−0.2277 (3)	3.2 (1)
N(3)	0.3235 (5)	0.4133 (4)	−0.2748 (3)	2.9 (1)
N(4)	0.2664 (5)	0.3041 (4)	−0.4518 (3)	2.9 (1)
N(11)	−0.2060 (9)	0.4550 (7)	0.0413 (5)	7.9 (2)
N(12)	0.1165 (9)	0.3488 (6)	0.2391 (5)	7.0 (2)
N(13)	0.3685 (8)	0.6389 (7)	0.3451 (4)	7.0 (2)
N(14)	0.316 (1)	0.8946 (7)	0.2564 (5)	10.4 (3)
N(15)	−0.084 (1)	0.7224 (7)	0.0257 (6)	9.8 (3)
C(1)	0.1713 (7)	0.0342 (5)	−0.3451 (4)	3.2 (1)
C(2)	0.0835 (7)	−0.0736 (5)	−0.3747 (5)	3.7 (1)
C(3)	0.0367 (8)	−0.1211 (5)	−0.3095 (5)	4.5 (2)
C(4)	0.0731 (8)	−0.0636 (5)	−0.2157 (5)	4.6 (2)
C(5)	0.1542 (8)	0.0457 (5)	−0.1845 (4)	4.2 (2)
C(6)	0.2068 (7)	0.0945 (4)	−0.2479 (4)	2.9 (1)
C(7)	0.3927 (7)	0.2622 (5)	−0.1499 (4)	3.4 (1)
C(8)	0.4603 (8)	0.3743 (5)	−0.1340 (4)	3.6 (1)
C(9)	0.4274 (7)	0.4467 (5)	−0.1912 (4)	3.4 (1)
C(10)	0.2881 (6)	0.4809 (5)	−0.3391 (4)	3.2 (1)
C(11)	0.2638 (7)	0.5921 (5)	−0.3149 (4)	4.0 (1)
C(12)	0.2182 (7)	0.6426 (5)	−0.3866 (5)	5.0 (2)
C(13)	0.1912 (8)	0.5852 (6)	−0.4808 (5)	4.8 (2)
C(14)	0.2092 (7)	0.4745 (5)	−0.5068 (4)	4.0 (1)
C(15)	0.2594 (6)	0.4217 (5)	−0.4366 (4)	3.2 (1)
C(16)	0.3250 (7)	0.2437 (5)	−0.5183 (4)	3.2 (1)
C(17)	0.3233 (7)	0.1278 (5)	−0.5307 (4)	3.7 (1)
C(18)	0.2755 (7)	0.0595 (5)	−0.4785 (4)	3.2 (1)
C(19)	0.4585 (9)	0.2034 (6)	−0.0771 (5)	4.8 (2)
C(20)	0.5241 (9)	0.5637 (5)	−0.1586 (5)	4.6 (2)
C(21)	0.4012 (8)	0.2984 (6)	−0.5791 (4)	4.7 (2)
C(22)	0.2978 (8)	−0.0618 (6)	−0.5061 (5)	4.7 (2)
C(23)	−0.0942 (9)	0.4845 (7)	0.0948 (5)	5.4 (2)
C(24)	0.1368 (8)	0.6156 (6)	0.1996 (4)	4.8 (2)
C(25)	0.0887 (9)	0.4229 (6)	0.2096 (5)	5.0 (2)
C(26)	0.0474 (8)	0.5115 (6)	0.1683 (4)	4.5 (2)
C(27)	0.2693 (7)	0.6300 (6)	0.2819 (4)	4.3 (2)
C(28)	0.125 (1)	0.7125 (6)	0.1681 (5)	5.9 (2)
C(29)	0.004 (1)	0.7158 (7)	0.0893 (5)	7.1 (2)
C(30)	0.305 (1)	0.1086 (9)	0.1473 (8)	11.3 (3)
C(31)	0.232 (1)	0.8144 (7)	0.2173 (5)	7.6 (3)

^{a} Estimated standard deviations in the last significant figure are given in parentheses. B values for anisotropically refined atoms are given in the form of the isotropic equivalent thermal parameter defined as $(4/3)[a^2B(1,1) + b^2B(2,2) + c^2B(3,3) + ab(\cos\gamma)B(1,2) + ac(\cos\beta)B(1,3) + bc(\cos\alpha)B(2,3)]$.

The structure amplitudes were obtained after the usual Lorentz and polarization reduction and converted to an absolute scale by least squares. No correction for absorption was applied.

Solution and Refinement of the Structure. The structure was solved by conventional Patterson and Fourier methods and refined by full-matrix least squares. After all non-hydrogen atoms were refined with anisotropic thermal parameters, all the hydrogen atoms were located from a difference Fourier synthesis (from 0.30 to 0.59 e.Å^{-3}). The final difference Fourier map was flat showing residual peaks not exceeding 0.40 e.Å^{-3}. Scattering factors and anomalous dispersion coefficient were taken from ref 18. All the computations were performed by using the SHELX-76 package of crystallographic program.[19] The final atomic parameters are given in Table II, relevant bond distances are given in Table III, and selected angles are given in Table IV.

Results and Discussion

Reactions of Complexes 1 ([[Mo($R_2C_{22}H_{20}N_4$)]$_2$]) with TCNE. Treatment of the diamagnetic dinuclear complex $[Mo(C_{22}H_{22}N_4)]_2$ (**1a**) (Figure 1) with TCNE (CH_3CN, room temperature,

(18) *International Tables for Crystallography*; Kynoch: Birmingham, England, 1974; Vol. IV.

(19) Sheldrick, G. M. *SHELX 76, Program for Crystal Structure Determinations*; University of Cambridge: Cambridge, England, 1976.

Table III. Significant Bond Distances (Å) with Esd's in Parentheses for $[MoO(C_{22}H_{22}N_4)][C_3(CN)_5]\cdot CH_2Cl_2$ (**3a**)

	Molybdenum Environment		
Mo(1)–N(1)	2.041 (4)	Mo(1)–N(2)	2.038 (5)
Mo(1)–N(3)	2.041 (4)	Mo(1)–N(4)	2.034 (4)
Mo(1)–O	1.670 (3)		
	Macrocyclic Ligand		
N(1)–C(1)	1.414 (6)	N(1)–C(18)	1.334 (6)
N(2)–C(6)	1.417 (6)	N(2)–C(7)	1.339 (7)
N(3)–C(9)	1.332 (7)	N(3)–C(10)	1.424 (6)
N(4)–C(15)	1.424 (6)	N(4)–C(16)	1.337 (6)
C(1)–C(2)	1.390 (7)	C(1)–C(6)	1.414 (7)
C(2)–C(3)	1.367 (8)	C(3)–C(4)	1.361 (9)
C(4)–C(5)	1.381 (8)	C(5)–C(6)	1.373 (7)
C(7)–C(8)	1.392 (7)	C(7)–C(19)	1.500 (9)
C(8)–C(9)	1.387 (8)	C(9)–C(20)	1.513 (7)
	Pentacyanopropenide Anion		
N(15)–C(29)	1.125 (12)	C(24)–C(28)	1.390 (9)
C(24)–C(26)	1.359 (8)	C(24)–C(27)	1.480 (9)
C(28)–C(29)	1.435 (12)	C(28)–C(31)	1.430 (11)
C(26)–C(25)	1.422 (9)	C(26)–C(23)	1.443 (10)
N(14)–C(31)	1.126 (10)	N(12)–C(25)	1.133 (8)
N(11)–C(23)	1.107 (9)	N(13)–C(27)	1.128 (8)

Table IV. Selected Angles (deg) with Esd's in Parentheses for $[MoO(C_{22}H_{22}N_4)][C_3(CN)_5]\cdot CH_2Cl_2$ (**3a**)

	Molybdenum Environment		
N(1)–Mo(1)–N(2)	77.9 (2)	N(1)–Mo(1)–N(3)	138.2 (2)
N(1)–Mo(1)–N(4)	87.2 (2)	N(1)–Mo(1)–O	110.1 (2)
N(2)–Mo(1)–N(3)	86.3 (2)	N(2)–Mo(1)–N(4)	137.0 (2)
N(2)–Mo(1)–O	112.8 (2)	N(3)–Mo(1)–N(4)	78.5 (2)
N(3)–Mo(1)–O	111.6 (2)	N(4)–Mo(1)–O	110.3 (2)
Mo(1)–N(1)–C(1)	104.5 (3)	Mo(1)–N(1)–C(18)	129.2 (3)
Mo(1)–N(2)–C(6)	104.6 (3)	Mo(1)–N(2)–C(7)	130.2 (3)
Mo(1)–N(3)–C(10)	103.8 (3)	Mo(1)–N(3)–C(9)	130.6 (4)
Mo(1)–N(4)–C(15)	105.1 (3)	Mo(1)–N(4)–C(16)	129.8 (4)
	Macrocyclic Ligand		
C(1)–N(1)–C(18)	126.3 (4)	C(6)–N(2)–C(7)	125.1 (5)
C(9)–N(3)–C(10)	125.4 (4)	C(15)–N(4)–C(16)	124.9 (4)
N(1)–C(1)–C(2)	126.8 (5)	N(1)–C(1)–C(6)	113.7 (4)
N(2)–C(6)–C(1)	114.2 (4)	N(2)–C(6)–C(5)	125.8 (5)
N(2)–C(7)–C(8)	122.2 (5)	N(2)–C(7)–C(19)	121.8 (5)
N(3)–C(9)–C(8)	122.2 (5)	N(3)–C(9)–C(20)	120.7 (5)
N(3)–C(10)–C(11)	125.7 (5)	N(3)–C(10)–C(15)	114.6 (4)
N(4)–C(15)–C(10)	113.5 (5)	N(4)–C(15)–C(14)	125.5 (5)
N(4)–C(16)–C(17)	121.5 (4)	N(4)–C(16)–C(21)	121.3 (5)
N(1)–C(18)–C(17)	122.8 (5)	N(1)–C(18)–C(22)	120.6 (5)
	Pentacyanopropenide Anion		
C(28)–C(24)–C(26)	131.0 (8)	C(28)–C(24)–C(27)	113.7 (6)
C(26)–C(24)–C(27)	115.2 (6)	C(24)–C(28)–C(29)	122.1 (8)
C(24)–C(28)–C(31)	119.7 (8)	C(29)–C(28)–C(31)	118.1 (7)
C(24)–C(26)–C(25)	120.5 (7)	C(24)–C(26)–C(23)	123.2 (7)
C(25)–C(26)–C(23)	116.3 (6)	N(12)–C(25)–C(26)	176.7 (8)
N(13)–C(27)–C(24)	178.3 (7)	N(11)–C(23)–C(26)	173.3 (9)
N(15)–C(29)–C(28)	175 (1)		

1:1 ratio) gives a brown solution. After a few minutes, this solution displays a typical ESR spectrum, which consists of two signals assignable to the previously known $[\{Mo(C_{22}H_{22}N_4)\}_2]^{\bullet+}$ radical cation[12] and the $TCNE^{\bullet-}$ radical anion[20] respectively (Figure 2). Both are indicative of a single electron transfer from the inorganic complex to the organic group in agreement with the redox potential values for $([\{Mo(C_{22}H_{22}N_4)\}_2]^{\bullet+}/[\{Mo(C_{22}H_{22}N_4)\}_2])$, $E = -0.42$ V, and for $TCNE/TCNE^{\bullet-}$, $E = -0.21$ V (reference Fc^+/Fc, C_6H_5CN, 0.1 M Bu_4NPF_6, 200 $mV\cdot s^{-1}$).

At this stage, the cationic dinuclear complex $[\{Mo(C_{22}H_{22}N_4)\}_2]^{\bullet+}$ $[TCNE]^{\bullet-}$ (**2a**) may be readily obtained by concentration of the solution; it shows in CH_3CN an ESR spectrum similar to that of the solution while its IR spectrum clearly reveals the presence of the $TCNE^{\bullet-}$ anion [ν(CN) (cm^{-1}) = 2183 s, 2144 m].

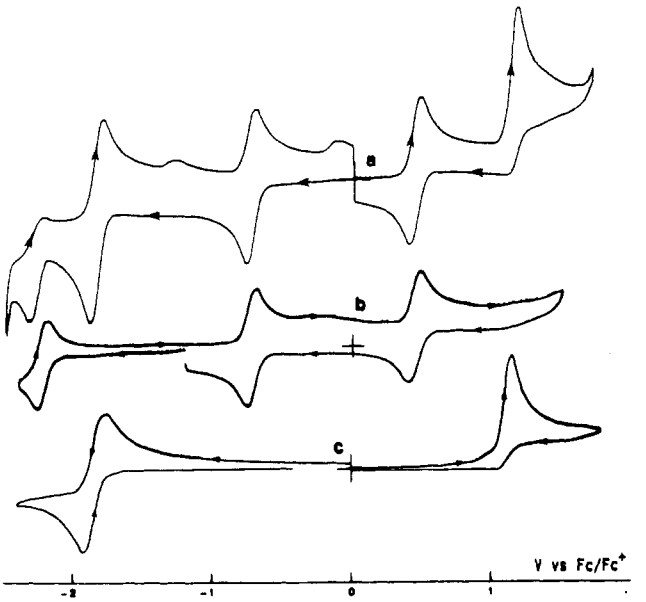

Figure 3. Cyclic voltammetry of (a) complex **3a** ($[MoO(C_{22}H_{22}N_4)][C_3(CN)_5]\cdot CH_2Cl_2$) (b) complex **4a** $[MoO(C_{22}H_{22}N_4)]$, and (c) $Et_4N[C_3(CN)_5]$ [benzonitrile solution; 0.1 M Bu_4NPF_6; glassy-carbon electrode; scan rate 100 $mV\cdot s^{-1}$].

The ESR spectrum of the above solution shows a clear evolution with time. While the two signals decrease and finally disappear, a new signal indicative of a $S = {}^1/_2$ molybdenum-centered radical [$g_{iso} = 1.958$; $A_{iso}(^{95}Mo,^{97}Mo) = 34.9$ G] appears in the spectrum and progressively increases, indicating formation of a new paramagnetic species.

Under a dinitrogen atmosphere, this species, **3a**, may be obtained in an almost pure state from acetonitrile solution by using a large excess of TCNE [TCNE:**1** = 4] while similar reactions conducted in the presence of air allow isolation of pure samples of **3a**. The crystal structure determination (see below) unequivocally shows that **3a** may be formulated as the unexpected oxomolybdenum(V) complex $[MoO(C_{22}H_{22}N_4)][C_3(CN)_5]$. The presence of the MoO unit in **3a**, confirmed by analysis of the IR spectrum [ν(MoO) = 950 cm^{-1}], clearly suggests the intervention of oxygen or water as does the presence of the 1,1,2,3,3-pentacyanopropenide $[(NC)_2C{-}C(CN){-}C(CN)_2]^-$ anion. Formation of this anion from TCNE has been previously observed.[21-24] It has been suggested to arise from reaction of TCNE with dioxygen or from hydrolysis of TCNE in the presence of a base B[21] according to

$$2C_2(CN)_4 + B + 2H_2O \rightarrow BH^+ + [C_3(CN)_5]^- + CO_2 + 3HCN$$

Although formation of complex **3a** from **1a** and TCNE seems to involve water or oxygen, it is noteworthy that this experiment is reproducible; **3b** and **3c**, analogues of **3a** with substituted $R_2C_{22}H_{20}N_4^{2-}$ ligands (**3b**, R = CH_3; **3c**, R = Cl; see Figure 1), have been obtained from the corresponding **1b** and **1c** dinuclear complexes by a similar procedure. Complex **3d** (R = CO_2CH_3) has not been prepared in this way since, presumably for steric reasons, we have been unable to obtain the dinuclear derivative **1d**. The oxocation of **3d** is prepared by electrochemical oxidation of the tetracarbonylmolybdenum(0) complex $[Mo(CO)_4(R_2C_{22}H_{22}N_4)]$ as we previously reported for **3a**;[16] it is noteworthy that careful analysis of the electrochemical data indicated that

(20) Phillips, W. F.; Rowell, J. C.; Weissman, S. I. *J. Chem. Phys.* **1960**, *33*, 626.

(21) Middleton, W. J.; Little, E. L.; Coffman, D. D.; Engelhardt, V. A. *J. Am. Chem. Soc.* **1958**, *80*, 2795.

(22) (a) Jensen, W. P.; Jacobson, R. A. *Inorg. Chim. Acta* **1981**, *50*, 189. (b) Bertolasi, V.; Gilli, G. *Acta Crystallogr.* **1983**, *C39*, 1252.

(23) Miller, J. S.; Calabrese, J. C.; Rommelmann, H.; Chittipeddi, S. R.; Zhang, J. H.; Reiff, W. M.; Epstein, A. J. *J. Am. Chem. Soc.* **1987**, *109*, 769.

(24) Webster, O. W.; Mahler, W.; Benson, R. E. *J. Am. Chem. Soc.* **1962**, *84*, 3678.

Table V. Cyclic Voltammetry Characteristics of the Redox Systems of the Inorganic Cations $[MoO(R_2C_{22}H_{20}N_4)]^+$ at a Platinum Disk Electrode (Referenced to the Fc^+/Fc System)[a,b]

solvent	R	$E^{R_2}_{1/2}$, V	ΔE_p, V	$E^{R_1}_{1/2}$, V	ΔE_p, V	$E^{O_1}_{1/2}$, V	ΔE_p, V
PhCN	CH_3	−2.31	0.180	−0.77	0.075	+0.39	0.095
PhCN	H	−2.22	0.090	−0.73	0.070	+0.44	0.090
PhCN	Cl	−2.06	0.070	−0.59	0.070	+0.51	0.110
PhCN	CO_2CH_3	−2.00	0.090	−0.55	0.090	+0.57	0.140
THF	CH_3	−2.15	0.100	−0.68	0.070	+0.40	0.100
THF	H	−2.07	0.095	−0.60	0.065	+0.50	0.140
THF	Cl	−1.90	0.090	−0.42	0.060	+0.62	0.140

[a] Supporting electrolyte: Bu_4NPF_6 (0.1 M). Scan rate: 0.1 $V\cdot s^{-1}$. [b] For all complexes **3**, two other redox processes are observed at −1.81 and 1.17 V. They are respectively associated with a reduction and an oxidation of the pentacyanopropenide anion (see Figure 3). [c] Further reduction observed at $E^{R_3}_{1/2}$ = −2.40 V, ΔE_p = 0.160 V.

residual water in benzonitrile was the source of oxygen.[16]

Electrochemical Studies of Complexes 3 ($[MoO(R_2C_{22}H_{20}N_4)][C_3(CN)_5]$). Cyclic voltammetry (CV) of complexes **3** in benzonitrile (0.1 M Bu_4NPF_6 as electrolyte support; scan rate 100 $mV\cdot s^{-1}$) reveals five redox processes (Figure 3; Table V). Separate CV study of $Et_4N[C_3(CN)_5]$ clearly indicates that two of them are associated with the $[C_3(CN)_5]^-$ anion (Figure 3), and therefore only three redox processes, two reductions and one oxidation, may be attributed to the inorganic cation. For the first reduction ($E_{1/2}$ from −0.77 V for **3b** to −0.55 for **3d**; $E_{1/2}$ values vs Fc^+/Fc) and the oxidation ($E_{1/2}$ from 0.39 V for **3b** to 0.57 V for **3d**) processes, the ratios between anodic and cathodic peak currents, $i_{pa}:i_{pc}$, are unity and independent of scan rate (from 5 to 500 $mV\cdot s^{-1}$). Plots of i_p $[=(i_{pa} + i_{pc})/2]$ vs $v^{1/2}$ (v for scan rate, $mV\cdot s^{-1}$) are linear, and potential separation between the anodic and cathodic peaks varies from 140 to 60 mV, while $E_{1/2}$ values are constant within an accuracy of ±3% regardless of scan rate variation. We refer, therefore, to each of these redox processes as reversible one-electron transfer without any coupled chemical reaction. The second reduction process ($E_{1/2}$ from −2.31 for **3b** to −2.00 V for **3d**) is only quasi-reversible.

The variations in half-wave potentials of electrochemical redox reactions of complexes **3** may be readily attributed to the variation of the electron-donating or electron-withdrawing characteristics of the substituents R of the macrocyclic ligand (Figure 1). As expected, the $E_{1/2}$ values given in Table V clearly show that the presence of withdrawing substituents favors both reductions and disfavors the oxidation process. Hammett plots of E vs $2\sigma_p$ are given in Figure 4.

In order to corroborate the number of electrons exchanged at the different redox steps and to determine the exact site (metal or ligand) associated with each redox process, different controlled-potential electrolysis and coulometry experiments have been performed.

Reduction of complex **3a** ($[MoO(R_2C_{22}H_{20}N_4)][C_3(CN)_5]$) (R = H) in benzonitrile (2.2 10^{-3} M solution, 0.1 M Bu_4NPF_6) was first performed electrochemically at −1.0 V vs Fc^+/Fc. The intensity of the ESR signal of **3a** decreases as the electrolysis proceeds and completely disappears after 2.5 h of electrolytic reduction without any new signal being observed. After this time, a charge very close to 1 faraday pmol has been consumed. The solutions of this $1e^-$ reduction product are stable when kept under a dinitrogen atmosphere. They do not undergo any electrochemically or spectrophotometrically detectable transformation and show a UV–visible spectrum that does not exhibit any absorption assignable to d–d transition. Taken with the disappearance of the ESR spectrum, this strongly suggests that the one-electron reduction occurs at the central metal atom [Mo(V)/Mo(IV)].

When similar reduction is carried out at −2.3 V, the starting green solution becomes first yellow and then orange. A plot of the electrolysis current i versus time converges toward an asymptotic value. After the electrolysis is stopped, the voltammogram of the solution at a rotating disk electrode indicates that the reduction process at −2.22 V has not been affected while the ESR spectrum does not show any signal assignable to a molybdenum-centered radical but exhibits a signal that clearly indicates reduction of the pentacyanopropenide diamagnetic anion $[C_3(CN)_5]^-$ into the radical dianion $[C_3(CN)_5]^{\cdot 2-}$ (Figure 5). Obviously, the second reduction process observed during the electrolysis experiments involves the 1,1,2,3,3-pentacyanopropenide anion.

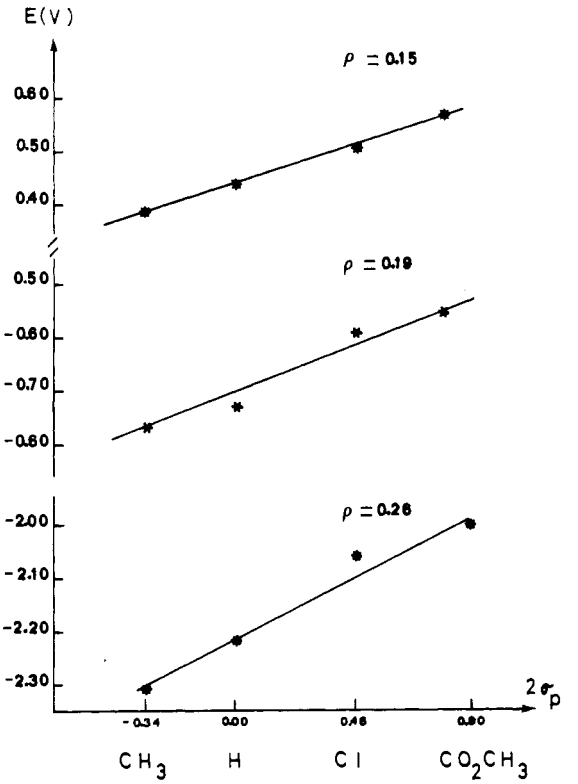

Figure 4. Hammett plots of E vs $2\sigma_p$ illustrating the dependence of redox potentials of the $[MoO(R_2C_{22}H_{20}N_4)]^+$ cations on σ_p.

When the electrolysis of **3a** is now performed at +0.8 V vs Fc^+/Fc, oxidation takes place. After 2.5 h of electrolysis, current intensity reaches a limiting value. The voltammogram at the rotating disk electrode obtained as quickly as possible (about 3 min) after the electrolytic reduction has been stopped indicates that only about two-thirds of the starting complex **3a** exists in the oxidized state. This voltammogram in fact shows a rapid change in the solution, which about 1 h after the interruption of the electrolysis has returned to its starting state even when kept under a dry nitrogen atmosphere. This behavior clearly indicates that a chemical reaction is coupled with the electrochemical reaction; this chemical process is thought to be slow since it cannot be detected on the time scale of the CV.

Attempts to obtain a UV–visible spectrum of the 1-electron oxidation product and to determine the site of oxidation were made by coupling UV–visible spectroscopy with the electrochemical measurements as follows. The potential was progressively increased (from 0.00 to 1.10 V at 2 $mV\cdot s^{-1}$) and absorption variations versus time were recorded at the maximum of absorption of the d–d transitions of **3a** (λ = 660 nm, ϵ = 800 $M^{-1}\cdot cm^{-1}$; see below). Unexpectedly, the absorption begins to increase when the potential reaches 0.7 V and stabilizes at ca. 1.0 V. At the end of the electrolysis, when the potential is kept at 1.1 V, the UV–visible

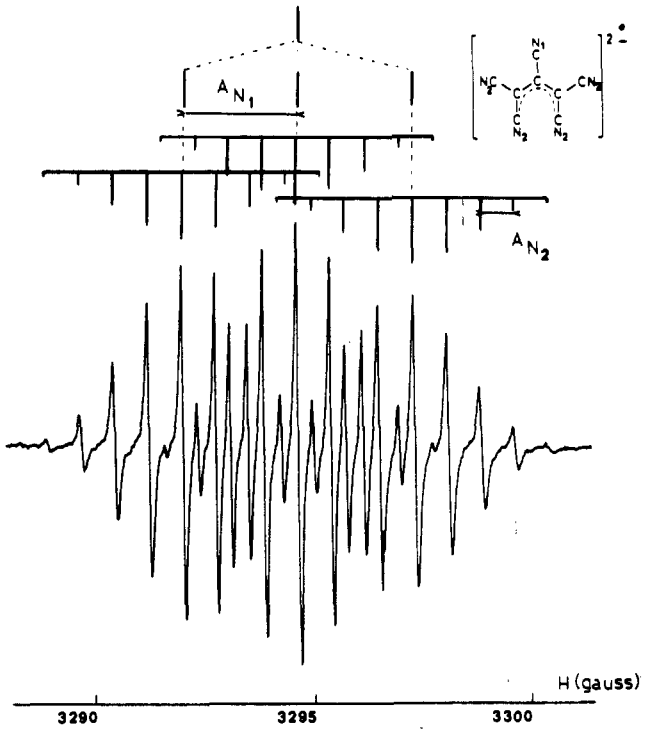

Figure 5. ESR spectrum of a THF solution of complex **3a** ($[MoO(C_{22}H_{22}N_4)][C_3(CN)_5]\cdot CH_2Cl_2$) after electrolysis at −2.2 V vs Fc^+/Fc. The observed spectrum corresponds to the radical dianion $[C_3(CN)_5]^{\bullet 2-}$ (g_{iso} = 2.0027; A_{N1} = 2.63 G; A_{N2} = 0.79 G).

spectrum exhibits a broad and slightly asymmetric absorption in the d–d transition range (λ = 672 nm, ϵ = 3100 $M^{-1}\cdot cm^{-1}$). This clearly suggests that oxidation takes place on the macrocyclic ligand and not on the metal since Mo(VI) has a d^0 configuration. It is noteworthy that a few minutes after the potential has been cut off, regeneration of the spectrum of the starting complex **3a** is again observed, corroborating that a chemical reaction is coupled with the electrochemical reaction.

Chemical Reductions of Complexes 3 ($[MoO(R_2C_{22}H_{20}N_4)][C_3(CN)_5]$). In THF solution and at room temperature, treatment of **3a** (R = H) with cobaltocene in a 1:1 ratio results in the reaction

$$\underset{\mathbf{3a}}{[MoO(C_{22}H_{22}N_4)][C_3(CN)_5]} + [Co(C_5H_5)_2] \rightarrow \underset{\mathbf{4a}}{[MoO(C_{22}H_{22}N_4)]} + [Co(C_5H_5)_2][C_3(CN)_5]$$

This affords the molecular complex **4a** in an almost quantitative yield. Complex **4a** is very air-sensitive, even in the solid state. Its air sensitivity precludes the obtaining of analytical data, and its formulation as an oxomolybdenum(IV) complex was deduced from (i) NMR data (the sharpness of the peaks is typical of a diamagnetic substance), (ii) IR data [ν(MoO) = 940 cm^{-1}] and (iii) CV data (this species displays CV behavior similar to that of its cationic congener **3a** with the exception that the process at −0.73 V now corresponds to an oxidation) (Figure 3).

It is noteworthy that an oxomolybdenum(IV) complex analogous to **4a** has been previously reported by Hashimoto et al.,[25] obtained by reaction of molybdenum hexacarbonyl with the unsubstituted dibenzotetraaza[14]annulene ligand in DMF.

Treatment in the dark of **4a** with the oxidizing reagent $[(Br-C_6H_4)_3N][SbCl_6]$ (THF, room temperature) afford in 70% yield a green powder that on the basis of ESR, IR, and UV–visible data has been formulated as the hexachloroantimonate salt, i.e. $[MoO(R_2C_{22}H_{20}N_4)][SbCl_6]$ (**5a**) (R = H).

By contrast with the above-mentioned reduction of **3a** with cobaltocene, reduction of **3a** under similar experimental conditions (THF solution, room temperature) but now using an excess of Na/Hg, affords a paramagnetic species. Unexpectedly, this species has been shown to be the dinuclear radical anion **1a**$^{\bullet -}$ ($[\{MoO(R_2C_{22}H_{20}N_4)\}_2]^{\bullet -}$) (R = H) by comparison of its ESR spectrum with that of an authentic sample prepared by reduction of **1a** with Na/Hg, as previously reported.[12]

Reaction of 3a with HCl. In THF solution, dry HCl reacts with **3a** ($[MoO(R_2C_{22}H_{20}N_4)][C_3(CN)_5]$) (R = H) to afford the new complex **6a** as a green powder in 88% yield. The IR spectrum of **6a** clearly exhibits an ν(MoO) absorption at 960 cm^{-1}, but does not show any absorption assignable to ν(CN) and ν(MoCl) vibrations. Formulation of **6a** as the cationic complex $[MoO(R_2C_{22}H_{20}N_4)]Cl$ rather than neutral $[MoO(R_2C_{22}H_{20}N_4)Cl]$ is also supported by the CV data, which are identical with those of the $[MoO(R_2C_{22}H_{20}N_4)]^+$ cation of **3a**.

Crystal Structure of 3a ($[MoO(R_2C_{22}H_{20}N_4)][C_3(CN)_5]\cdot CH_2Cl_2$) (R = H). The asymmetric unit of **3a** (Figure 6) contains one $[MoO(C_{22}H_{22}N_4)]^+$ cation, a pentacyanopropenide anion $[C_3(CN)_5]^-$, and a dichloromethane solvate. In the cation (Figure 7), the molybdenum atom has a slightly distorted square-pyramidal coordination; the oxygen atom is axially coordinated while the four nitrogen atoms of the macrocyclic ligand occupy the equatorial positions.

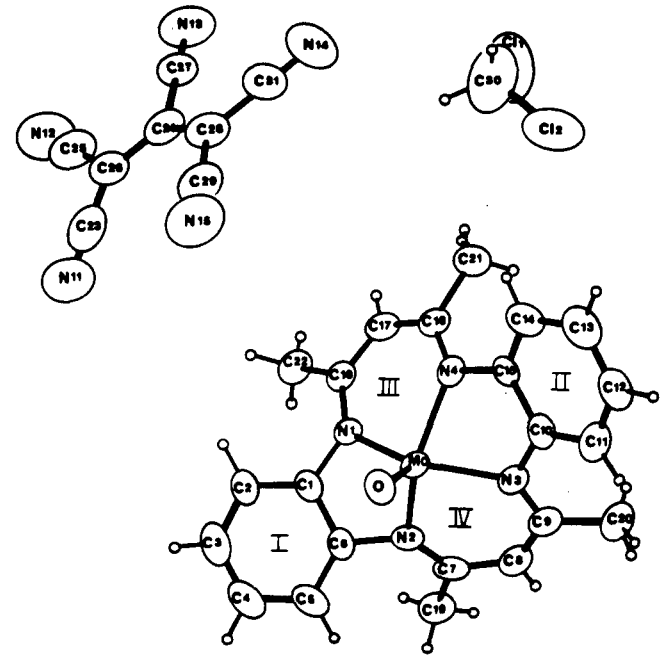

Figure 6. View of the structure of complex **3a** ($[MoO(C_{22}H_{22}N_4)][C_3(CN)_5]\cdot CH_2Cl_2$) showing the atom-labeling scheme. Non-hydrogen atoms are shown as 50% thermal ellipsoids. The hydrogen atoms have been arbitrarily assigned artificially small thermal parameters. Selected dihedral angles (deg) are as follows: I–II, 45.2 (2); I–III, 39.7 (3); I–IV, 140.5 (2); II–III, 39.2 (2); II–IV, 138.7 (2); III–IV, 112.4 (2) where I, II, III, and IV are respectively the best mean planes C(1)···C(6), C(10)···C(15), N(1)–C(18)–C(17)–C(16)–N(4), and N(2)–C(7)–C(8)–C(9)–N(3). Uncertainties in the last significant digit are shown in parentheses.

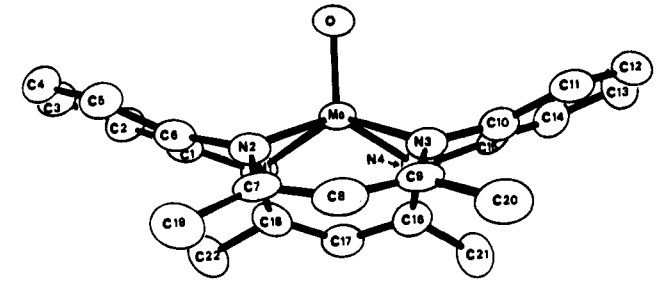

Figure 7. View of the $[MoO(C_{22}H_{22}N_4)]^+$ cation of **3a**. λ Hydrogen atoms are omitted for clarity. Non-hydrogen atoms are shown as 50% thermal ellipsoids.

(25) Hashimoto, M.; Iwashita, H.; Gondo, K.; Sakata, K. *Kyushu Kogyo Daigaku Kenkyu Hokoku, Kogaku* **1985**, *51*, 49.

Table VI. Spin-Hamiltonian Parameters for $[MoO(R_2C_{22}H_{20}N_4)]^+$ Cations[a]

complex	R	g_{iso}	A_{iso}	g_{xx}	g_{yy}	g_{zz}	A_{xx}	A_{yy}	A_{zz}	$\langle g \rangle$	$\langle A \rangle$
3a	H	1.9574	35.4	1.9714	1.9583	1.9338	22.5	27.0	60.0	1.9545	36.5
3b	CH_3	1.9573	34.7	1.9777	1.9650	1.9385	25.0	26.0	58.0	1.9604	36.3
3c	Cl	1.9581	35.6	1.9691	1.9575	1.9438	22.5	27.0	64.0	1.9568	37.8
c	CO_2Me	1.9567	35.4	1.9760	1.9653	1.9324		*b*		1.9579	*b*
5a	H	1.9567	35.2	1.9654	1.9592	1.9365		*b*		1.9537	*b*

[a] All hyperfine tensor components are in G (throughout this paper 1 G = 10^{-4} T). Solvent = 2-methyltetrahydrofuran. Isotropic values refer to room-temperature spectra; anisotropic values refer to frozen-solution spectra run at 140 K. [b] Not determined. [c] $[MoO(R_2C_{22}H_{20}N_4)]^+$ (R = CO_2Me) solutions prepared by controlled-potential electrolyses of benzonitrile solutions of the corresponding tetracarbonyl complex $[Mo(CO)_4(R_2C_{22}H_{22}N_4)]$ (see Experimental Section).

The MoO distance, 1.670 (3) Å, compares well with those reported for other oxomolybdenum(V) complexes.[26] The molybdenum atom is displaced by 0.737 (1) Å from the N_4 mean coordination plane toward the oxygen, a displacement similar to that observed in the corresponding titanyl complex $[TiO(C_{22}H_{22}N_4)]$[27] (0.754 Å) but slightly longer than that in the vanadyl derivative $[VO(C_{22}H_{22}N_4)]$[28] (0.673 Å).

The Mo–N distances [2.034 (4)–2.041 (4) Å] average 2.038 (4) Å, which is slightly shorter than that in $\mathbf{1a}^{\bullet+}$ (2.07 Å)[12] but much longer than the ideal distance (1.85–1.90 Å).[29]

As expected, the macrocyclic ligand exhibits its usual double-saddle-shaped geometry, mainly due to the steric interactions of the methyl groups of the 2,4-pentanediiminato chelate rings with the benzenoid ring.[27,30] Each of the benzenoid rings is tipped up toward the oxygen by about 23° relative to the N_4 plane, while the six-membered chelate rings are both tipped downward by about 34°. As in other complexes with this ligand, the interatomic distances within the macrocyclic moiety indicate a strong delocalization broken by the four single C–N bonds of the *o*-phenylenediamine residues (average 1.42 Å).

The pentacyanopropenide anion has a slightly distorted C_{2v} symmetry, the most important deviation concerning the two C–C distances of the allyl skeleton [1.359 (8) and 1.390 (9) Å]. Bond length and angle values agree well with those previously reported for this anion.[22,23] It is noteworthy that the C–CN distance of the central carbon atom [1.480 (9) Å] is longer than the four corresponding distances associated with the terminal carbon atoms [from 1.422 (9) to 1.443 (10) Å; average 1.435 (10) Å].

ESR Study of Bonding in Complexes 3. All of the ESR spectra of complexes **3** in 2-methyltetrahydrofuran (fluid solution at room temperature or frozen solution at ca. 140 K) consist of a signal arising from the $I_{Mo} = 0$ isotopes (^{94,96,98,100}Mo, natural abundance ca. 75%) and a signal arising from hyperfine coupling with the $I_{Mo} = {}^5/_2$ isotopes (^{95,97}Mo, natural abundance ca. 25%). The small difference (<2%) in magnetic moments of the last two isotopes[31] does not give rise to observable splittings. No superhyperfine features due to the coupling of the unpaired electron with the ^{15}N nuclei ($I = 1$) have been observed.

The room-temperature spectra can be described by using the isotropic spin Hamiltonian (1), where all the symbols have their usual meanings.

$$\hat{H}_{iso} = g_{iso}\beta\hat{H}\cdot\hat{S} + A_{iso}\hat{I}\cdot\hat{S} \quad (1)$$

The measured values are listed in Table VI. Obviously, the nature of the R substituent on the macrocycle has little influence on the ESR properties. It is worthy of note that the observed hyperfine coupling value (ca. 35 G) is significantly lower than that in the porphyrin molybdenum(V) complexes [MoO(porph)X] (ca. 50 G).[32]

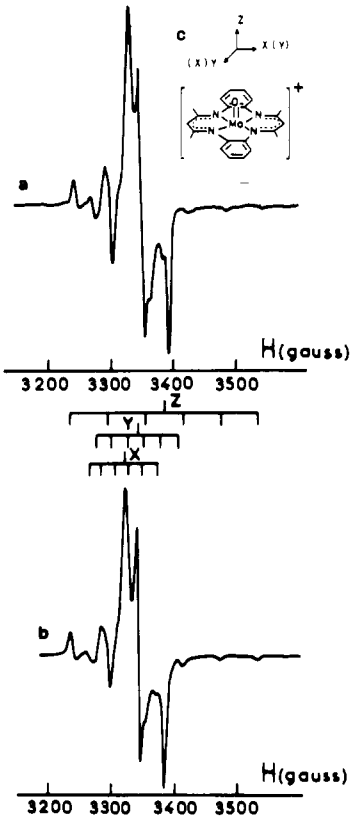

Figure 8. ESR spectra of complex **3a** ($[MoO(C_{22}H_{22}N_4)][C_3(CN)_5]\cdot C-H_2Cl_2$) at 140 K in 2-methyltetrahydrofuran: (a) experimental spectrum; (b) simulated spectrum. The coordinate system is shown in (c).

Straightforward analyses of the frozen-solution spectra can be made by assuming that the ligand field around Mo^{5+} has a C_{2v} symmetry in agreement with the results of the X-ray study. This point group symmetry requires all g and A tensor axes to be coincident.[33] Since the quadrupolar interactions at the central atom appear to be very small, the spin-Hamiltonian can be written in the diagonal form (2).

$$\hat{H} = g_{xx}\beta\hat{H}_x\cdot\hat{S}_x + g_{yy}\beta\hat{H}_y\cdot\hat{S}_y + g_{zz}\beta\hat{H}_z\cdot\hat{S}_z + A_{xx}\hat{S}_x\cdot\hat{I}_x + A_{yy}\hat{S}_y\cdot\hat{I}_y + A_{zz}\hat{S}_z\cdot\hat{I}_z \quad (2)$$

Iterative computation of the frozen-solution spectra leads to calculated spectra in very good agreement with the experimental spectra (Figure 8). The final values of the spin-Hamiltonian parameters are listed in Table VI. There is no major change in any of the parameters for the complex studies. It is noteworthy that the results indicate only a weak C_{2v} perturbation of the dominant C_{4v} symmetry, in agreement with the slightly asymmetric nature of the macrocyclic ligand.

(26) Holm, R. H. *Chem. Rev.* **1987**, *87*, 1401 and references therein.
(27) Yang, C. H.; Ladd, J. A.; Goedken, V. L. *J. Coord. Chem.* **1988**, *19*, 235.
(28) Yang, C. H.; Ladd, J. A.; Goedken, V. L. *J. Coord. Chem.* **1988**, *18*, 317.
(29) Goedken, V. L.; Pluth, J. J.; Peng, S. M.; Bursten, B. *J. Am. Chem. Soc.* **1976**, *98*, 8014.
(30) See, for instance: (a) Goedken, V. L.; Peng, S. M.; Molin-Norris, J.; Park, Y. *J. Am. Chem. Soc.* **1976**, *98*, 8391. (b) Tsutsui, M.; Bobsein, R. L.; Cash, G.; Pettersen, R. *Inorg. Chem.* **1979**, *18*, 758 and references therein.
(31) See, for instance: Cotton, F. A.; Pedersen, E. *Inorg. Chem.* **1975**, *14*, 399.
(32) Matsuda, Y.; Murakami, Y. *Coord. Chem. Rev.* **1988**, *92*, 157 and references therein.
(33) Scullane, M. I.; Taylor, R. D.; Minelli, M.; Spence, J. T.; Yamanouchi, K.; Enemark, J. H.; Chasteen, N. D. *Inorg. Chem.* **1979**, *18*, 3213.

Table VII. UV-Visible Spectral Data for Complexes **3a** and **6a** in Benzonitrile

complex	E_{max}, 10^3 cm^{-1} (ϵ, 10^3 M^{-1}·cm^{-1})						
3a	14.0 (0.8)[a]	15.3 (1)[a]	20.3 (2.5)[b]	23.9[c]	25.3[c]	27.5 (41)[d]	30.1[d]
5a	14.1 (0.8)[a]	15.4 (1.2)[a]	20.3 (2.3)[b]	23.7 (3.6)[d]		27.7 (29)[d]	30.8 (13)[d]

[a] d ← d transition. [b] Uncertain assignment. [c] Band associated with the $[C_3(CN)_5]^-$ anion by comparison with the spectrum of $Et_4N[C_3(CN)_5]$. [d] Charge-transfer band.

More precise information can be obtained about electron distribution within complexes **3** if the spin-Hamiltonian parameters are expresses as functions of the molecular-orbital coefficients.

In the crystal-field approximation, the weak effective C_{2v} perturbation mixes the molybdenum $4d_{x^2-y^2}$ and $4d_{z^2}$ orbitals so that in the ground state with the coordinate system shown in Figure 8, the unpaired electron is in an orbital described by the linear combination

$$\psi = a|d_{x^2-y^2}\rangle + b|d_{z^2}\rangle \quad (3)$$

with $a^2 + b^2 = 1$ and $a^2 \gg b^2$.

In ligand-field theory, this metal ion orbital combines with a ligand orbital combination of appropriate symmetry (A_1), and in the ground state, the unpaired electron must be described by

$$\psi_{A_1} = \alpha[a|d_{x^2-y^2}\rangle + b|d_{z^2}\rangle] + \alpha''|L_{A_1}\rangle \quad (4)$$

Other magnetically important antibonding molecular orbitals corresponding to excited states are given by (5).

$$\psi_{A_1} = \alpha'[a'|d_{x^2-y^2}\rangle + b'|d_{z^2}\rangle] + \alpha'''|L_{A_1}\rangle$$
$$\psi_{A_2} = \beta|d_{xy}\rangle + \beta'|L_{A_2}\rangle$$
$$\psi_{B_1} = \gamma|d_{xz}\rangle + \gamma'|L_{B_1}\rangle$$
$$\psi_{B_2} = \delta|d_{yz}\rangle + \delta'|L_{B_2}\rangle \quad (5)$$

Spin–orbit coupling, Zeeman interactions, and hyperfine coupling all perturb these basic functions. If the matrix elements of these interactions are equated with those of the spin-Hamiltonian (2) then the spin-Hamiltonian parameters can be expressed as functions of the coefficients of the molecular orbitals (4) and (5). For an unpaired electron in a C_{2v} ligand field, these functions have been shown[34] to be

$$g_{xx} = g_e - \frac{2a(a + 2\sqrt{3}b)\alpha^2\gamma^2\lambda}{E_{xz} - E_{x^2-y^2}} \quad (6)$$

$$g_{yy} = g_e - \frac{2a(a - 2\sqrt{3}b)\alpha^2\delta^2\lambda}{E_{yz} - E_{x^2-y^2}} \quad (7)$$

$$g_{zz} = g_e - \frac{8a^2\alpha^2\beta^2\lambda}{E_{xy} - E_{x^2-y^2}} \quad (8)$$

$$A_{xx} = P\left[-K + \frac{2}{7}a^2\alpha^2 - \frac{4\sqrt{3}}{7}ab - (g_e - g_{xx}) + \frac{1}{14}\frac{3a + \sqrt{3}b}{a - \sqrt{3}b}(g_e - g_{yy}) - \frac{1}{7}\frac{b}{a}(g_e - g_{zz})\right] \quad (9)$$

$$A_{yy} = P\left[-K + \frac{2}{7}a^2\alpha^2 + \frac{4\sqrt{3}}{7}ab - (g_e - g_{yy}) + \frac{1}{14}\frac{3a - \sqrt{3}b}{a + \sqrt{3}b}(g_e - g_{xx}) + \frac{1}{7}\frac{b}{a}(g_e - g_{zz})\right] \quad (10)$$

$$A_{zz} = P\left[-K - \frac{4}{7}a^2\alpha^2 - \frac{1}{14}\frac{3a + \sqrt{3}b}{a - \sqrt{3}b}(g_e - g_{yy}) - \frac{1}{14}\frac{3a - \sqrt{3}b}{a + \sqrt{3}b}(g_e - g_{xx}) - (g_e - g_{zz})\right] \quad (11)$$

when the small b^2 terms are neglected. In these expressions, K is the isotropic Fermi contact term, α is the spin–orbit coupling constant of the Mo ion in the valence state appropriate to the complex and $P = 2.0023\beta_e\beta_N g_N\langle d_{x^2-y^2}|r^{-3}|d_{x^2-y^2}\rangle$. In order to take into account the screening effect of the negatively charged ligand, all calculations have been made with P and λ values corresponding to the Mo^{3+} formal oxidation state ($P = -0.0055$ cm^{-1}; $\lambda = 820$ cm^{-1}) as is usually done for molybdenum(V) complexes.[35]

The measured ESR parameters (Table VI) together with eqs 3, 9, 10, and 11 allow us to calculate a^2, b^2, α^2 and K. Iterative calculations have been made by assuming the A_{xx}, A_{yy}, and A_{zz} constants are positive since the nuclear magnetic moments for the ^{95,97}Mo isotopes are negative[35] and by attributing the largest hyperfine splitting to A_{zz} by comparison with previous work on oxomolybdenum(V) complexes. It is not possible, with the ESR data alone, to determine either the relative signs of a and b, or which of the in-plane **g** tensor components should be attributed to g_{xx} or g_{yy}. According to our x and y assignments, as indicated in Table VI, it follows that a and b should have opposite signs. Interchange of x and y axes would lead to the same sign for a and b without any variation of their absolute values.

The values found for **3a**, $|a| = 0.999$, $|b| = 0.028$, $\alpha = 0.77$, and $K = 0.56$, are indicative of a strong delocalization of the unpaired electron onto the ligands in the ground state. They show this electron is only ca. 60% localized on the metal, almost entirely in the $d_{x^2-y^2}$ orbital, since the contribution of the d_{z^2} orbital appears extremely weak. The Fermi isotropic interaction K value of 0.56 is much lower than the 0.9 value commonly accepted in the $[MoOX_5]^{2-}$ anion (X = Cl, F),[35] but agrees well with that recently reported for the $[MoO(SPh)_4]^-$ anion (from 0.58 to 0.65 depending on the solvent).[36]

In order to obtain the values of the molecular orbital coefficients for the excited states, assignments of the band maxima in the UV–visible absorption spectra of complexes **3** are needed. Since the pentacyanopropenide anion has strong absorptions in the range studied, assignment has been made also for the hexachloroantimonate complex **5a** (Table VII). In this spectrum, an intense band can be seen around 28 000 cm^{-1} while an asymmetric and broad absorption, actually arising from the overlap of two absorptions, appears near 15 000 cm^{-1} (Figure 9). Comparison with previous work,[37] molar extinction coefficient values, and consistency with the ESR data indicate that the two absorptions near 15 000 cm^{-1} are attributable to d ← d transitions and should be assigned as follows:

$$14\,100\ \text{cm}^{-1} \quad B_1|XZ\rangle \leftarrow A_1|X^2 - Y^2\rangle$$
$$15\,400\ \text{cm}^{-1} \quad B_2|YZ\rangle \leftarrow A_1|X^2 - Y^2\rangle$$

Evaluation of the coefficients γ^2 and δ^2 according to eqs 7 and 8 give $\gamma^2 = 0.53$ and $\delta^2 = 0.57$, which indicate a strong participation of the ligand orbitals in the two first excited states.

Attempts To Characterize the Oxotungsten Analogues of Complexes 3. As described above, the oxomolybdenum(V) com-

(34) (a) Abragam, A.; Pryce, M. H. L. *Proc. R. Soc. London, A* **1951**, *205*, 135. (b) McGarvey, B. R. *Transition Metal Ion Chemistry*; Carlin, R. L., Ed.; Dekker: New York, 1966; Vol. 3, p 89. (c) Hitchman, M. A.; Belford, R. L. *Inorg. Chem.* **1969**, *8*, 958.
(35) (a) De Armond, K.; Garrett, B. B.; Gutowski, H. S. *J. Chem. Phys.* **1965**, *42*, 1019. (b) Manoharan, P. T.; Rogers, M. T. *J. Chem. Phys.* **1968**, *49*, 5510 and references therein.
(36) Al Mowali, A. H.; Kuder, W. A. A.; Bader, M. J.; Majead, N. N. *J. Coord. Chem.* **1981**, *11*, 1.
(37) See, for instance: Stiefel, E. I. *Prog. Inorg. Chem.* **1977**, *22*, 1 and references therein.

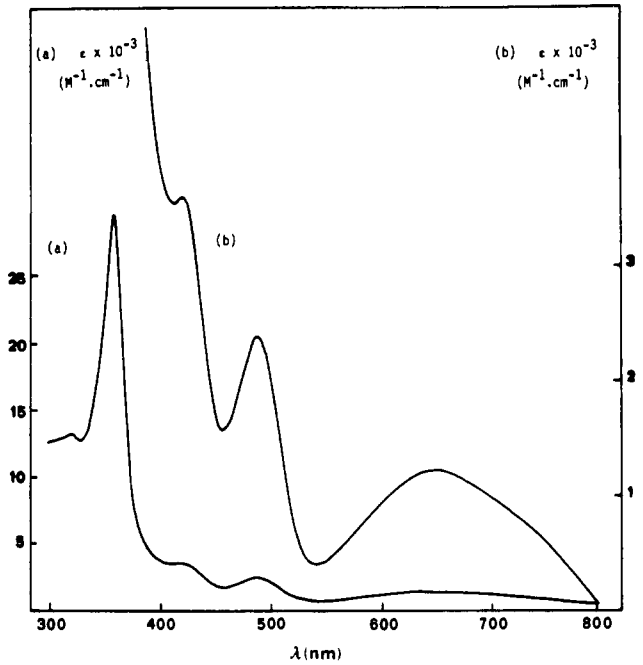

Figure 9. UV-visible spectrum of $[MoO(C_{22}H_{22}N_4)][SbCl_6]$ (**5a**) in benzonitrile.

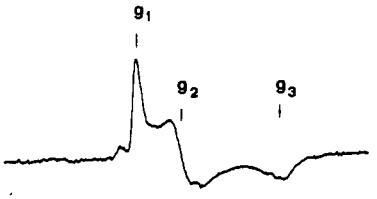

Figure 10. Frozen-solution ESR spectrum of the oxotungsten(V) cation $[WO(C_{22}H_{22}N_4)]^+$ (benzonitrile, 140 K): $g_1 = 1.875$, $g_2 = 1.842$, and $g_3 = 1.777$.

plexes $[MoO(R_2C_{22}H_{20}N_4)][C_3(CN)_5]$ (**3**) have been prepared from the dinuclear complexes $[\{Mo(R_2C_{22}H_{20}N_4)\}_2]$ (**1**), themselves obtained from the well-known molybdenum acetate $[Mo_2(acet)_4]$. The corresponding tungsten acetate has been described,[38] but it is not easily accessible and we have not been able, as yet, to prepare the ditungsten complexes analogous to **1**. Therefore an alternative strategy had to be used for the preparation of the oxotungsten(V) cations $[WO(R_2C_{22}H_{20}N_4)]^+$. The cation $[WO(C_{22}H_{22}N_4)]^+$ has been obtained by electrochemical oxidation at 0.77 V vs Fc^+/Fc of the carbonyl complex $[W(CO)_4(C_{22}H_{24}N_4)]$ in benzonitrile as previously described.[15] As for the corresponding molybdenum cations, the CV data indicate that this tungsten cation may undergo two reduction (−2.10 and −0.75 V) and one oxidation (0.25 V) processes. While no ESR spectrum is observed at room temperature, the frozen solution (benzonitrile, 140 K) gives a spectrum that is similar in shape to those of the Mo(V) analogues, but as observed earlier,[39] the line widths are here significantly broader (Figure 10). Because of the increased line width, the expected hyperfine splittings due to ^{183}W ($I = {}^1/_2$, natural abundance ca. 14%) are only partially resolved and precise A_W values have not been obtained. The three g values (see Experimental Section) associated with the orthorhombic symmetry are considerably lower than that of the molybdenum analogues because of stronger spin–orbit coupling.[39]

Concluding Remarks

The mononuclear oxymolybdenum(V) and -(IV) complexes **3**, **5**, and **4**, the quadruply molybdenum–molybdenum-bonded complex **1**, and the corresponding radical anions $\mathbf{1}^{\bullet-}$ constitute a unique system showing the following easy conversion:

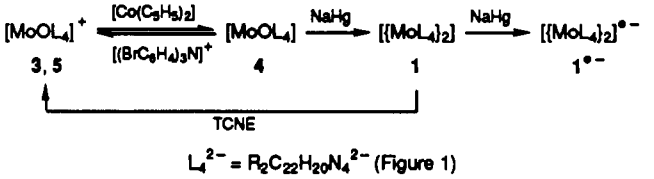

Note Added in Proof. While this work was in press, the starting dinuclear complex **1a** ($[\{Mo(C_{22}H_{22}N_4)\}_2]$) was experimentally and theoretically investigated by Cotton et al. (*Inorg. Chem.* **1990**, *29*, 4329). The crystal structure determination confirms the structure shown in Figure 1 with two saddle-shaped ligands rotated 90° to each other and a Mo—Mo distance of 2.175 (1) Å.

Acknowledgment. We thank the DRET for financial support of this research, the MEN for a studentship (J.M.G.), and Dr. D. Mandon (Strasbourg, France) for valuable discussions. We are particularly indebted to Drs. Y. Le Mest and M. L'Her (Brest, France) for helpful discussions and for the use of electrochemical equipment. It is a pleasure to acknowledge the assistance of Dr. S. A. R. Knox (Bristol, U.K.) for valuable discussions and a careful reading of the manuscript.

Supplementary Material Available: A table of positional parameters for hydrogen atoms and tables of displacement parameters and torsion angles (3 pages); a list of observed and calculated structure factor amplitudes (10 pages). Ordering information is given on any current masthead page.

(38) Santure, D. J.; Huffman, J. C.; Sattelberger, A. P. *Inorg. Chem.* **1985**, *24*, 371.

(39) Rice, C. A.; Kroneck, P. M. H.; Spence, J. T. *Inorg. Chem.* **1981**, *20*, 1996 and references therein.